

Processing Deficits in Primary Visual Cortex of Amblyopic Cats

Kerstin E. Schmidt, Wolf Singer and Ralf A. W. Galuske

J Neurophysiol 91:1661-1671, 2004. First published 10 December 2003; doi:10.1152/jn.00878.2003

You might find this additional info useful...

This article cites 87 articles, 33 of which can be accessed free at:

<http://jn.physiology.org/content/91/4/1661.full.html#ref-list-1>

This article has been cited by 1 other HighWire hosted articles

Comparison of contrast-response functions from multifocal visual-evoked potentials (mfVEPs) and functional MRI responses

Jason C. Park, Xian Zhang, John Ferrera, Joy Hirsch and Donald C. Hood

J Vis, October 22, 2008; 8 (10): .

[\[Abstract\]](#) [\[Full Text\]](#) [\[PDF\]](#)

Updated information and services including high resolution figures, can be found at:

<http://jn.physiology.org/content/91/4/1661.full.html>

Additional material and information about *Journal of Neurophysiology* can be found at:

<http://www.the-aps.org/publications/jn>

This information is current as of April 13, 2011.

Processing Deficits in Primary Visual Cortex of Amblyopic Cats

Kerstin E. Schmidt, Wolf Singer, and Ralf A. W. Galuske

Max-Planck-Institut für Hirnforschung, 60528 Frankfurt, Germany

Submitted 8 September 2003; accepted in final form 5 December 2003

Schmidt, Kerstin E., Wolf Singer, and Ralf A. W. Galuske. Processing deficits in primary visual cortex of amblyopic cats. *J Neurophysiol* 91: 1661–1671, 2004. First published December 10, 2003; 10.1152/jn.00878.2003. Early esotropic squint frequently results in permanent visual deficits in one eye, referred to as strabismic amblyopia. The neurophysiological substrate corresponding to these deficits is still a matter of investigation. Electrophysiological evidence is available for disturbed neuronal interactions in both V1 and higher cortical areas. In this study, we investigated the modulation of responses in cat V1 to gratings at different orientations and spatial frequencies (SFs; 0.1–2.0 cycles/°) with optical imaging of intrinsic signals. Maps evoked by both eyes were well modulated at most spatial frequencies. The layout of the maps resembled that of normal cats, and iso-orientation domains tended to cross adjacent ocular dominance borders preferentially at right angles. Visually evoked potentials (VEPs) were recorded at SFs ranging from 0.1 to 3.5 cycles/° and revealed a consistently weaker eye for the majority of squinting cats. At each SF, interocular differences in VEP amplitudes corresponded well with differences in orientation response and selectivity in the maps. At 0.7–1.3 cycles/°, population orientation selectivity was significantly lower for the weaker eye in cats with VEP differences compared with those with no VEP amplitude differences. In addition, the cutoff SF, above which gratings no longer induced orientation maps, was lower for the weaker eye (≥ 1.0 cycles/°). These data reveal a close correlation between the loss of visual acuity in amblyopia as assessed by VEPs and the modulation of neuronal activation as seen by optical imaging of intrinsic signals. Furthermore, the results indicate that amblyopia is associated with altered intracortical processing already in V1.

INTRODUCTION

Strabismus refers to a misalignment of the optical axes of the two eyes that, in humans, occurs either congenitally or is acquired in the course of various pathologies. When strabismus is present during early development binocular fusion and stereopsis become severely impaired. Frequently, diplopia is avoided by using only one eye at a time for fixation. However, in many cases, one eye is permanently suppressed from conscious vision and develops perceptual deficits referred to as strabismic amblyopia. Behaviorally, these deficits consist of reduced visual acuity expressed as reduced contrast sensitivity and reduced spatial resolution as well as reduced Vernier acuity (Levi and Klein 1985), temporal instability (Altmann and Singer 1986), spatial distortions of the images (Hess and Holliday 1992; Hess et al. 1978; Lagreze and Sireteanu 1991; Pugh 1958; Sireteanu et al. 1993a), and crowding (Levi and Klein 1983, 1985).

Cats and monkeys with a surgically induced squint angle can serve as a model of the human disorder as well as a model of

experience-dependent postnatal development of neuronal connectivity. In cats, the lack of binocular vision is accompanied by a drastic reduction of binocular neurons in primary visual cortex (e.g., Hubel and Wiesel 1965), an enhanced eye-specific segregation of geniculocortical afferents into ocular dominance domains (Löwel 1994; Shatz et al. 1977), and decreased interocular interactions through long-range intrinsic connections (Löwel and Singer 1992; Schmidt et al. 1997; Trachtenberg and Stryker 2001). While the lack of binocular neurons has been suggested to form the basis of disturbed stereoscopic vision in monkeys (Crawford et al. 1983) and humans (Hohmann and Creutzfeldt 1975), the neurophysiological substrate of the visual acuity deficit remains less clear.

In primary visual cortex, neurons driven by the deviating eye are as numerous as those driven by the normal eye (cat: Chino et al. 1983; Mower et al. 1982; Roelfsema et al. 1994; Singer et al. 1980; human: Horton and Hocking 1996; macaque: Blakemore and Vital-Durand 1992; Kiorpes et al. 1998) and exhibit no or slightly disturbed spatial response properties (Blakemore and Vital-Durand 1992; Chino et al. 1983; Crewther and Crewther 1990; Eschweiler and Rauschecker 1993; Freeman and Tsumoto 1983; Kiorpes et al. 1998; Roelfsema et al. 1994; Singer et al. 1979, 1980). However, response latencies to visual stimulation of the deviating eye (Eschweiler and Rauschecker 1993) and to electrical stimulation of its optic nerve (Freeman and Tsumoto 1983) are clearly prolonged compared with the normal eye. Compatible with this finding and in accordance with reduced behavioral performance, synchronization of responses among neurons driven by that eye is reduced at high spatial frequencies (Roelfsema et al. 1994). Recent functional MRI (fMRI) studies of strabismic amblyopic humans revealed functional deficits also at the level of V1 (Algaze et al. 2002; Barnes et al. 2001; Goodyear et al. 2000, 2002).

To gain a comprehensive insight into the relation between the processing of visual signals in V1 and the acuity deficit of amblyopic animals, we correlated orientation preference maps at different spatial frequencies (SFs) obtained by optical imaging of intrinsic signals with visually evoked potentials (VEP) in squinting cats. Optical imaging allows for the visualization of spatially distributed neuronal activity over large areas, and in addition, is capable of displaying not only neuronal spiking (Thompson et al. 2003), but also subthreshold activity (Das and Gilbert 1995; Toth et al. 1996). VEPs, in turn, are known to correspond to behaviorally evaluated interocular differences in visual acuity in strabismic cats (von Grünau and Singer 1980) and humans (Arden et al. 1974; Holopigian et al. 1991; Levi

Address for reprint requests and other correspondence: K. E. Schmidt, Max-Planck-Institut für Hirnforschung, Deutschordenstraße 46, 60528 Frankfurt, Germany (E-mail: schmidt@mpih-frankfurt.mpg.de).

The costs of publication of this article were defrayed in part by the payment of page charges. The article must therefore be hereby marked "advertisement" in accordance with 18 U.S.C. Section 1734 solely to indicate this fact.

and Harwerth 1978; Lombroso et al. 1969; Manny and Levi 1982; Spekreijse et al. 1971).

METHODS

Animals

Three normally raised and 11 esotropic strabismic cats of our institute's colony were included in this study. At the age of 2.5–15 mo, VEPs were evoked in primary visual cortex with phase-reversing gratings at different SFs and compared with orientation preference maps that were obtained with optical imaging again at different SFs and separately for the two eyes. In two strabismic cats, the ocular dominance distribution was evaluated by electrophysiological single-unit recordings at the end of the imaging experiment. All animal experiments have been performed according to the German Law on the Protection of Animals and corresponding European Communities Council Directive (86/609/EEC).

Induction of squint

Anesthesia consisted of an intramuscular injection of ketamine hydrochloride (10 mg/kg, Ketanest, Parke-Davis) and xylazine hydrochloride (2.5 mg/kg, Rompun, Bayer). Convergent squint was surgically induced in nine kittens at the age of 11–16 days (A5, 31 days) by transecting the tendon of the lateral rectus muscle of one eye (see Table 1). This procedure has been proven not to induce any deprivation effect or deficits in subcortical pathways (Crewther et al. 1985; for review, Rauschecker 1991). Subsequently, the ratio of the corneal reflex distance over the distance between the pupils was monitored weekly from the age of 2–8 wk. To this end, each cat was restrained manually, and several flashlight snapshots of the animal's face were taken. The distances between the corneal reflexes and the pupils were measured on the photoprints. The ratio of the reflex distance over the pupillary distance can be taken as a reliable indicator of eye alignment (Olson and Freeman 1978; Sherman 1972; von Grünau 1979). The ratios measured were always in the range of 0.97–1.01 in all operated cats, indicating a successful induction of esotropia (Sireteanu et al. 1993b; von Grünau 1979). None of the cats had anisometropia >1 dpt at the time of the final optical imaging experiment.

Refraction of the eyes

The pupils were dilated, and accommodation was paralyzed by topical atropine (1%) application. The nictitating membrane was retracted with topical phenylephrinhydrochloride (1%). Corneae were

protected by contact lenses with an artificial pupil of 3 mm diam and with sufficient power to focus the eyes on the stimulation monitor (21 in, 100-Hz refresh rate, Hitachi CM815ET Plus) at a distance of 57 cm. Refraction was double-checked by two experimenters with a Rodenstock refractometer. When contact lenses were changed or eyes were cleaned with saline solution, topical anesthesia with proxymetacaine-hydrochloride was applied. The deviating eye was aligned on the monitor by means of a prism or slight abduction (Yin et al. 1983) to ensure equal visual stimulation conditions for both eyes.

Surgery and anesthesia for optical imaging and electrophysiology

Anesthesia was induced as described above (ketamine/xylazine), and after tracheal intubation and cannulation of a humeral vein, was maintained by ventilating the cat with a mixture of 70% N₂O–30% O₂ supplemented by 0.4–1% halothane (Hoechst). After completion of the surgery, animals were paralyzed for recording with a continuous infusion of pancuronium (0.3 mg/kg/h). The animal's head was fixed in a stereotaxic frame by means of a metal nut cemented onto the skull. The ECG, pulmonary pressure, and CO₂ content of the expired air were continuously monitored. End-tidal CO₂ was kept in the range of 3–4%, and rectal temperature was maintained in the range of 37–38°C. A craniotomy covering both hemispheres was performed between A6 and P13 (Horsley-Clarke), and a circular stainless steel chamber, 20 mm diam, was mounted onto the skull over the exposed region with dental cement (Paladur, Kulzer, Wehrheim, Germany). After removing the dura, the chamber was filled with silicone oil (Boss Products, Elisabethtown, KY) and sealed with a round glass coverslip. Additionally, three silver ball electrodes were implanted subdurally at the midline (Horsley-Clarke L0/P4) and laterally over both occipital cortices (L5/P6).

VEPs

Since visual acuity of the operated eye varies in adult strabismic cats (Roelfsema et al. 1994; Yin et al. 1983), all squinting cats and cat N1 were tested prior to optical imaging by means of VEPs. Amplitudes of VEPs are reduced for amblyopic eyes compared with normal companion eyes in cats (Freeman et al. 1983; Von Grünau and Singer 1980; Yin et al. 1983, 1994) and humans (Holopigian et al. 1991; Lombroso et al. 1969; Manny and Levi 1982). VEPs were recorded in anesthesia from three silver ball electrodes placed over visual cortex (L0/P4; L5/P6 bilaterally) using an acquisition system based on a PDP 11 computer (Digital VT 101). Individual trials lasted 1 s, during which phase-reversed (every 500 ms) vertical whole-field gratings

TABLE 1. Age of squint induction and map investigation; interocular differences in mean orientation map vector strength

| Cat | Squinting Eye | Age of Squint Induction | Functionally Weaker Eye | Age at Map Investigation | Protocol for Imaging | Mean Vector Strength Difference (%) |
|-----|---------------|-------------------------|-------------------------|--------------------------|------------------------|-------------------------------------|
| A1 | LE | 11d | | 194d | 7 SF, constant flicker | 0.27 |
| A2 | LE | 11d | | 265d | 7 SF, constant flicker | 0.61 |
| A3 | LE | 16d | LE | 125d | 7 SF, 4 deg/s | 18.5 |
| A4 | LE | 16d | LE | 88d | 7 SF, 4 deg/s | 18 |
| A5 | LE | 31d | RE | 102d | 7 SF, 4 deg/s | 15.2 |
| A6 | RE | 12d | RE | 110d | 7 SF, 4 deg/s | 16 |
| A7 | LE | 11d | LE | 180d | 7 SF, constant flicker | 22.7 |
| A8 | LE | 15d | LE | 116d | 7 SF, constant flicker | 15.9 |
| A9 | LE | 14d | LE | 219d | 7 SF, constant flicker | 23.1 |
| A10 | LE | 16d | LE | 64d | 0.5 cyc/deg, 4 deg/s | 22.2 |
| A11 | LE | 11d | LE | ~1.5y | 0.5 cyc/deg, 4 deg/s | 23.9 |
| N1 | | | | ~1.5y | 7 SF, constant flicker | 0.43 |
| N2 | | | | ~1y | 0.5 cyc/deg, 4 deg/s | 0.65 |
| N3 | | | | ~1y | 0.5 cyc/deg, 4 deg/s | 0.3 |
| MD | LE | 30d | LE | 36d | 0.5 cyc/deg; 4 deg/s | 66 |

SF, spatial frequency; LE, left eye; RE, right eye; constant flicker, flicker frequency was kept at 2 Hz.

(30 × 40 cm) at eight SFs (0.1, 0.4, 0.7, 1.0, 1.3, 2.0, 2.6, and 3.5 cycles/°) plus a control stimulus devoid of contours matching the average luminance of the grating (34.1 C/m²) were presented monocularly in random order at a distance of 57 cm. Gratings were presented at high contrast (93%) because amplitude differences between potentials evoked by different eyes are more pronounced at high contrast (Singer et al. 1980; Yin et al. 1983). One hundred repetitions per condition were averaged; each average contained the responses to two reversals. For quantification, the response to two reversals was summed. Latencies and sequences of peaks and troughs differed depending on the eye and tested SF (Arden et al. 1974; Snyder and Shapley 1979), and amplitudes varied in different cats (Yin et al. 1983). Therefore the largest evoked amplitude (difference between the 1st negative and 1st positive deflection) in an interval between 30 and 160 ms after each reversal was taken as an objective measurement of visual performance of the two eyes per SF (amplitude A2 in Singer et al. 1980). In Fig. 1, the amplitude means of two cats were plotted as relative units normalized to the largest amplitude per cat as a function of SF (Fig. 1). For quantification, the difference between the two eyes was expressed as the relative difference between mean amplitudes in percent of the respective larger amplitude (see also Yin et al. 1983). Differences were evaluated only in cases in which at least one grating evoked response was larger than the responses to the luminance-matched stimulus recorded within the same time period (noise level).

Optical imaging of intrinsic signals

Subsequently, orientation preference maps were visualized in V1 with optical imaging of intrinsic signals (for methodological details see Bonhoeffer and Grinvald 1993; Schmidt et al. 1997). Recording chambers centered on Horsley-Clarke coordinate P4 were filled with silicone oil and sealed with a glass coverslip. Signals were recorded with a cooled CCD camera system (System 2000, Digital Pixel; or Ora2001, Optical Imaging Europe, Munich, Germany) under illumination with light of a wavelength of 560 nm for surface images and of 620 nm for functional imaging. The camera was fitted with a lens system consisting of two 50-mm Nikon objectives and a 2× extender providing a 3.6 × 4.8-mm field of view at the resolution of 144 × 192

pixels. For functional imaging, the camera was focused at 600 μm below the pial surface.

Cats A1–A9 and N1 were monocularly stimulated with square-wave whole-field (30 × 40 cm) gratings of four different orientations (0, 45, 90, and 135°) moving in two directions at seven different SFs ranging from 0.1 to 2.0 cycles/° (total = 56 conditions); cats A10, A11, N2, and N3 were tested at 0.5 cycles/° only. Each condition was presented 32–40 times per stimulation block. Stimuli were presented in pseudo-randomized order in two protocols containing 32 (0.1, 0.4, 0.7, and 1.0 cycles/°) or 24 conditions (0.5, 1.3, and 2.0 cycles/°) because the acquisition system was limited to a maximum of 32 conditions. In each protocol, conditions were repeated eight times, and the two protocols were presented interleaved to keep the time between conditions of the same block short. Contrast was kept constant (93%), and mean luminance was 34.1 C/m²; drift velocity was either adapted to maintain the flicker frequency at 2 Hz or gratings drifted at 4 °/s (Table 1). Stimuli were presented for 3 s, and camera frames were collected during the entire stimulation period.

For quantitative analysis, signals were averaged by stimulus condition and divided by the average of all images in a given stimulation protocol (“cocktail blank”) and filtered using a high pass of 50 pixels and a low pass of 3 pixels. The two raw data blocks containing different spatial frequencies could not be merged because of overall offset brightness variations in the camera frames of different randomizations taken at different times. Because this problem could neither be overcome by cocktail blank nor blank normalization (unpublished observations), we economized recording time by using cocktail blank normalization. This procedure was appropriate since we were interested in relative differences between maps evoked by different eyes and not in absolute differences of signal strength.

Responses to the four stimulus orientations were vectorially summed for each pixel. For the orientation vector (tuning) strength, the length of the resulting vector per pixel was normalized to the sum of all four orientation responses giving values between 0 and 1 (0 for completely unmodulated pixels and 1 for pixels selectively responding to only one orientation). Vector strength was computed for the sum of single condition maps obtained with stimulation of one eye and one SF and pseudocolor-coded for illustration (Fig. 5). Vector

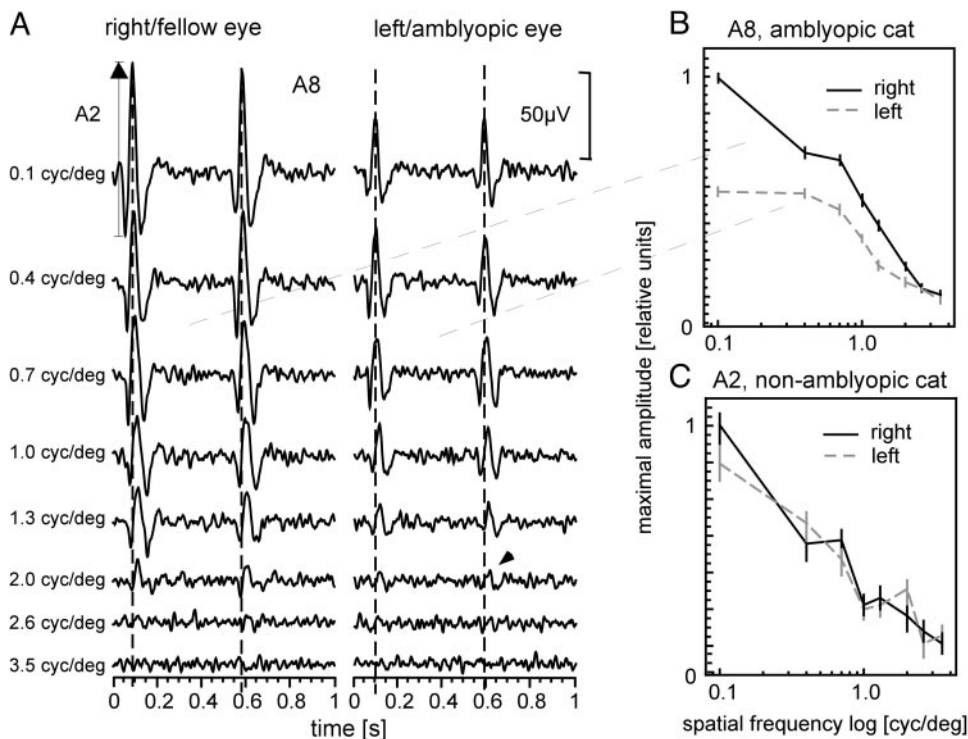


FIG. 1. Averaged visually evoked potentials (VEPs) of cat A8 (A and B) and cat A2 (C) during monocular stimulation with phase reversed square wave gratings. A: analog signal averaged from 100 trials recorded during 2 phase reversals (500 ms) through a silver ball electrode positioned over the vertex. Recordings lasted 1,000 ms and started with the onset of the 3rd of 6 phase reversals. Note that amplitudes A2 (Singer et al. 1980) evoked by stimulation of the left eye are consistently lower and latencies higher than those evoked by stimulation of the right eye. Amplitudes of peak A2 decline and latencies increase with increasing spatial frequency (SF) for both eyes. B and C: mean evoked maximal amplitudes (peak to trough, A2) in the interval of 80–150 ms after the phase reversal are displayed in relative units between noise level (0) and the maximal evoked amplitude in the overall data set (1) and plotted against the logarithm of the tested SF. Vertical bars represent SE in 100 trials. Left eye mean amplitudes are interconnected with the gray dashed line; right eye mean amplitudes with the black solid line. B: data depicted in A. Note that mean amplitudes ± SD are nonoverlapping for the 2 eyes in B but overlapping in C, although both cats underwent squint surgery.

(tuning) strength averaged over a region of interest void of large blood vessels was compared between both eyes for each SF. Relative interocular differences in percentage of the respective larger vector strength were compared for different SFs and different cats (hemispheres).

For further comparison, data obtained at 0.5 cycles/° in cat MD, which had been monocularly deprived for 1 wk at the age of 30 days, were analyzed (Galuske et al. 2000; see their Fig. 1). In cats A4, A5, and A7, both hemispheres were examined.

Since the number of neurons preferring vertical contours is reduced in amblyopic cats (Chino et al. 1983, 1991; Cynader et al. 1984; Singer et al. 1979), we investigated the relative size of the cortical territory devoted to the vertical orientation domains (0°). To this end, we split interocular vector strength differences at 0.5 cycles/° of all cats into four compartments (ct) according to the preference angle α per pixel: $\alpha + 45^\circ > ct \geq \alpha - 45^\circ$.

Analogous to cumulative spatial frequency maps introduced by Issa et al. (2000), ocular dominance distributions were computed from the maps generated through the respective eyes at a single SF. To this end, each pixel was assigned to the eye (and the SF) evoking the strongest response in the respective condition cocktail (32 or 24 conditions).

To characterize the local geometric relationship between iso-orientation domains and ocular dominance borders, we computed their intersection angles in maps obtained at 0.5 cycles/°. A detailed description of this method is given in Löwel et al. (1998).

Electrophysiological recordings

The ocular dominance distribution was additionally investigated by electrophysiological unit recordings in hemispheres ipsilateral to the operated eye in two cats (A7, 141 units; A8, 179 units) to estimate the possibility that our squint surgery had induced monocular deprivation. Extracellular activity was recorded with tungsten micro-electrodes, band-pass filtered from 1 to 3 KHz, and fed into a Schmitt trigger to threshold the signals. Thresholds were adjusted during stimulation with bars of different speed and orientation to isolate single-unit activity. Subsequently, ocular dominance was assessed acoustically during separate stimulation of the eyes with light bars produced by a hand-held projector. According to their ocular dominance, neurons were grouped into five classes (Gu and Singer 1993). Units that were driven exclusively by one eye were classified in groups 1 or 5 depending on whether they were dominated by the eye ipsilateral or contralateral to the recorded hemisphere. Units responding to both eyes but stronger to one eye were assigned to group 2 for ipsilateral eye dominance and group 4 for contralateral eye dominance. Units responding almost equally strong to both eyes were classified as group 3.

RESULTS

VEPs

In VEP measurements, responses with amplitudes higher than those obtained in the iso-luminant control condition could be detected up to SFs of 2.0–2.6 cycles/°. These cutoff frequencies are in agreement with a study of the development of VEPs in cats using similar stimulation (Freeman and Marg 1975). For the classification of visual deficits, averaged responses evoked from the two eyes were compared (Fig. 1A). In the following, a VEP data set is defined as a pair of averaged maximal responses evoked by stimulation of each eye at a certain SF and a certain electrode. Only data sets in which at least one of the two averaged responses was above noise level were included in the quantitative analysis. Data from different electrodes in the same cat were not pooled because interocular

amplitude differences varied slightly between hemispheres. Thus for the following classification of cats and statistics, only data from the vertex electrodes were compared. The normal control cat N1 revealed average amplitude differences of $18.3 \pm 6.8\%$ (SD) between the eyes at all evaluated SFs (0.1–2.0 cycles/°) and the means \pm SD of the two amplitude distributions were overlapping except at 0.1 cycles/°. The esotropic cats split into two groups (compare Fig. 1, B and C). The first group consisted of esotropic cats A1 and A2 and was classified as “nonamblyopic” (NA) because mean amplitude \pm SD intervals overlapped. The two cats revealed average amplitude differences of $19.4 \pm 13.0\%$ between visual potentials evoked through different eyes (Figs. 1C, 2, and 6B), and as in the normal cat, the eye through which higher amplitudes could be evoked was switching in a nonsystematic manner each eye leading in about 50% of the VEP data sets (see Fig. 1C). These observations indicate that neither cat A1 nor A2 had developed a consistently weaker eye after squint surgery. The second group consisted of cats A3–A11. In this group, amplitudes evoked by stimulation of the operated eye, and in cat 5 of the nonoperated eye, were lower than those evoked by the companion eye and had nonoverlapping mean amplitude \pm SD distributions in $93 \pm 7\%$ of the VEP data sets (Figs. 1, A and B, and 2). Mean amplitudes of responses evoked from the weaker eye were on average $48.9 \pm 26.9\%$ lower than those evoked by the companion eye. Therefore cats A3–A11 were classified as “amblyopic” (A). In all squinting cats, at least one eye evoked responses in the range of the normal cat. This excludes the development of bilateral amblyopia.

For statistical testing, mean inter-ocular amplitude differences at each electrode were compared between cat groups and separately for each investigated SF (Fig. 2). Amplitude differences between NA cats and the normal control were not different from each other (Mann-Whitney-U; $P = 0.41$) and were therefore treated as one NA/normal group for later processing. Distributions of mean amplitude differences were significantly different between NA/normal and A cats (Mann-Whitney-U; $P < 0.015$ for groups of 36 data sets at each of 5 tested SFs between 0.1–1.3 cycles/°). SFs higher than 1.3 cycles/° (2.0–3.5 cycles/°) were not statistically tested because amplitudes did not exceed the noise level in some data sets and because close to noise level relative interocular differences became

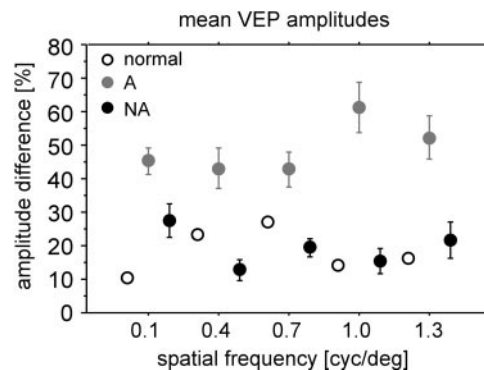


FIG. 2. Relative interocular difference between the means of maximal VEP amplitudes at the vertex electrode in normal (open circles), amblyopic esotropic (A, gray filled circles), and nonamblyopic esotropic cats (NA, black filled circles) plotted against tested SF. Distributions of the means in the normal/NA and in the A group are significantly different from each other at each SF ($P < 0.015$). Error bars = SE.

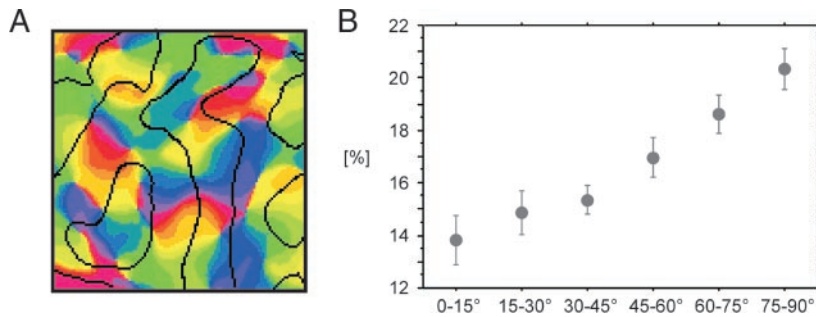


FIG. 3. A: superposition of ocular dominance borders and orientation domains in cat A7. B: intersection angles between ocular dominance borders and iso-orientation lines in 6 A and 2 NA cats. Right angles predominate.

large in both normal and strabismic data sets. Although the leading eye switched frequently in this group (Fig. 1C), differences in the NA/normal group were treated as uni-directional for conservative statistical treatment.

To exclude multiple comparison (more than 1 data set from the same cat), we also tested interocular amplitude differences pooled from all SFs within one cat. Also in this analysis, the distributions of the means were significantly different between NA/normal and A cats (Mann-Whitney-U: $P = 0.014$, $n = 12$).

Geometry of orientation preference maps

There was no difference in layout between orientation maps of normal, A, and NA esotropic strabismic cats at different SFs. Maps elicited by stimulation of the operated or nonoperated eye did not differ in shape and geometry of the domains. Intersection angles between ocular dominance borders and

iso-orientation lines were computed for A and NA cats that exhibited well-modulated maps for both eyes at 0.5 cycles/° ($n = 8$), which was the optimal stimulation frequency for area 17. Iso-orientation domains tended to cross ocular dominance borders continuously and intersect at right angles ($20.3 \pm 2.3\%$ in the group of 75–90°) in both NA and A cats as described previously for divergent and convergent NA cats (Fig. 3).

Orientation preference maps at different spatial frequencies

Since there was neither a qualitative nor a quantitative difference between maps obtained with fixed or adjusted drift velocity, data obtained with these different protocols were merged. In all cats tested at different SFs (A1–A9, N1), orientation domains in V1 could be elicited by stimulation of either eye at low SFs (≤ 0.7 –1.0 cycles/°; Figs. 4 and 5). However, as indicated by lower contrast in some maps, re-

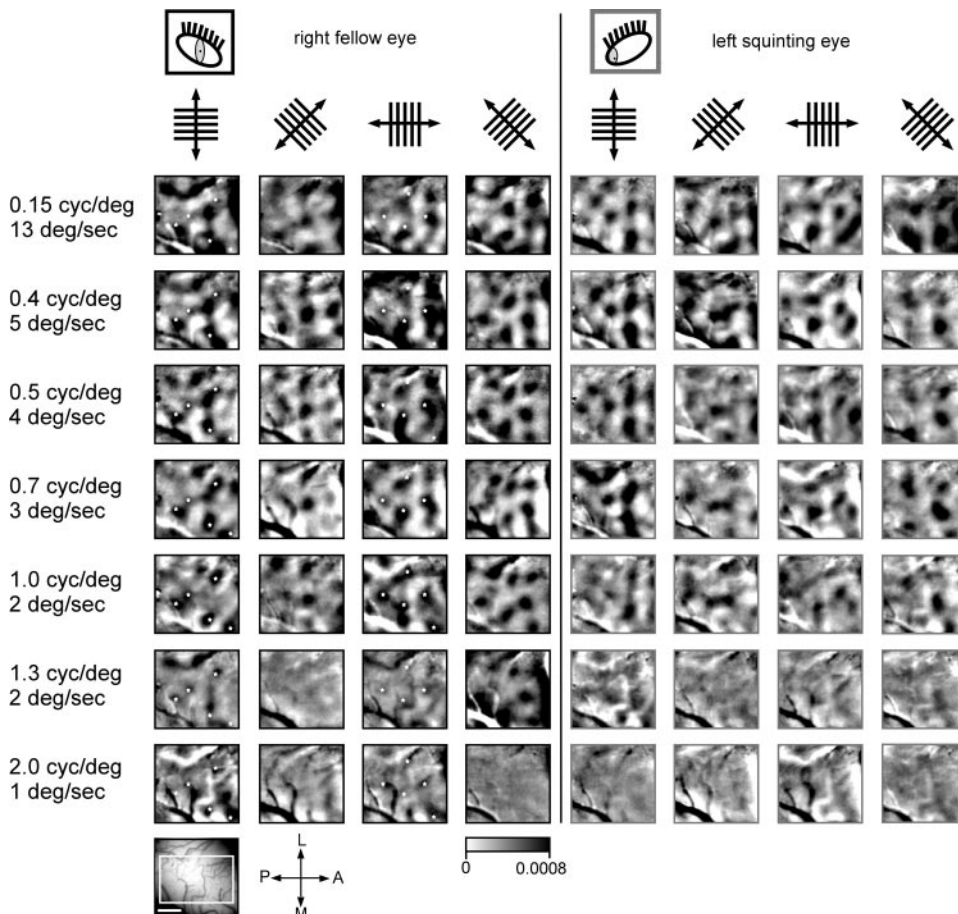


FIG. 4. Optically imaged single orientation preference maps of cat A7 (hemisphere ipsilateral to the squinting eye) obtained during monocular stimulation with moving square wave gratings of 4 orientations (top sketches relate to the entire column) and 7 different SFs with adjusted velocities (see METHODS, left values relate to entire row). All images were normalized to cocktail-blank and clipped at fixed values (range, 0.08%). Therefore all images can be compared in signal strength using the gray value bar at the bottom (black codes highest signal intensity). Bottom left corner: video image of the recorded area in 560 nm. Scale bar: 1 mm. L, lateral; A, anterior; M, medial; P, posterior. Note that modulated single condition maps can be observed for both eyes but that the signal strength is lower in maps obtained with left eye stimulation, especially at higher SFs.

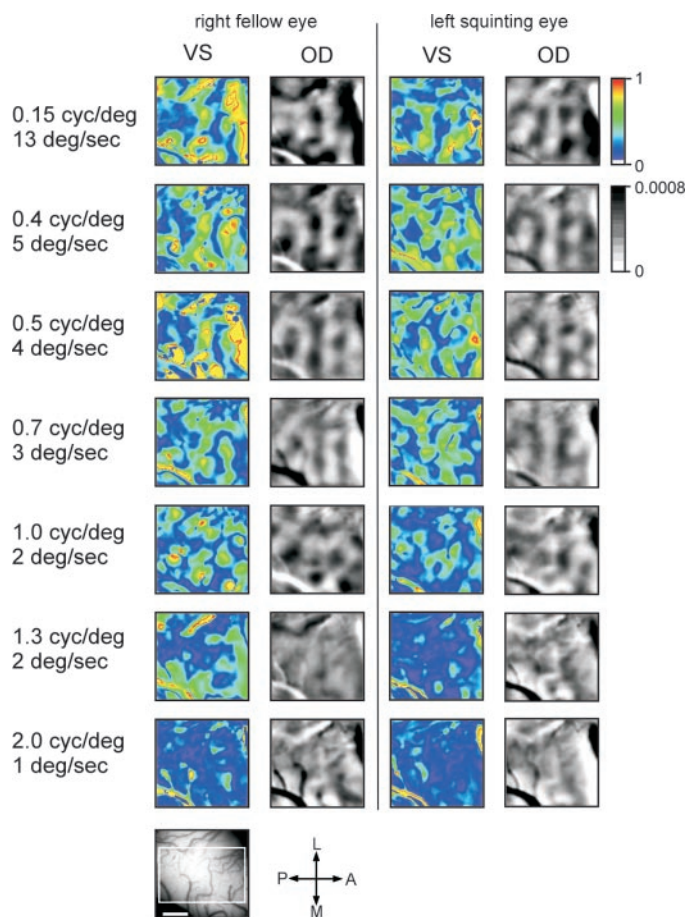


FIG. 5. Monocular vector strength (1st and 3rd column) and ocular dominance maps (obtained by summing up the cocktail-blank normalized single condition maps of 1 eye; 2nd and 4th column) of cat A7. The 4 different single orientation maps obtained by stimulation of 1 eye and a single SF (Fig. 3) were vectorially summed. Sum vector was normalized to the sum of all 4 vectors, and result is pseudo-color coded according to the scheme on the top right corner (highly selective: 1, unselective: 0, see METHODS). Signal range in the ocular dominance maps is coded according to the gray value bar on the right. Bottom left corner: video image of the recorded area in 460 nm. Scale bar: 1 mm. Cortical coordinates as in Fig. 4.

sponse strength for stimulation of the A eye was on average lower than for stimulation of the NA eye at all SFs (Fig. 4). This was not the case for NA cats. In the A cats, differences in the single condition maps became particularly pronounced at high SFs, and finally, maps were often no longer elicited through the A eye with high-frequency gratings (>1 cycles/ $^{\circ}$), whereas maps evoked through normal eyes were occasionally preserved ≤ 2.0 cycles/ $^{\circ}$.

As a quantitative parameter, we evaluated orientation vector strength (see METHODS), which reflects the orientation specific modulation of neuronal responses in the map. Although the parameter is normalized to the overall response, it is not completely independent of the signal-to-noise ratio and usually reflects both responsiveness and tuning strength. Thus in the majority of pixels, large vector strengths usually correlate with large response strengths and vice versa. Data collected at 2.0 cycles/ $^{\circ}$ were not included in the quantitative analysis because the induced vector strengths were sometimes very low, both in squinting and normal cats, in agreement with the lack of modulation in single condition maps (see Figs. 4 and 6A). They

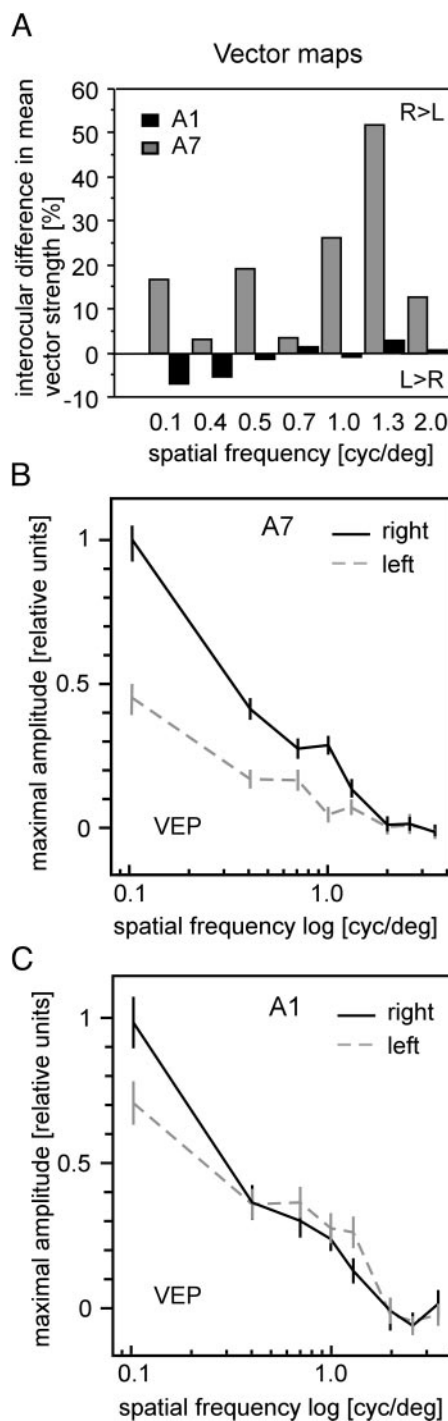


FIG. 6. Interoocular difference in average vector strength per pixel (A) and VEP amplitudes (B and C) of cats A1 and A7 in a large defined region of interest of the vector strength maps. A: relative difference in mean vector strength (per pixel) in a defined region of interest in the vector strength maps of cat A1 (black bars) and of cat A7 (gray bars, Fig. 3) plotted against tested SF. Negative differences indicate that the left squinting eye was stronger; positive differences indicate that the right nonsquinting eye was stronger. B and C: mean evoked amplitudes recorded at the vertex electrodes. Conventions as in Fig. 1. According to the VEPs, cat A7 (B) is categorized as A and cat A1 (C) as NA. Note that in agreement with interocular differences in map vector strength in A, cat A7 (B) reveals consistently larger VEP amplitudes of the right eye and cat A1 (C) reveals small VEP amplitude differences at all SFs.

were in the range of the deprived eye's vector strength of cat MD at 0.5 cycles/° (vector strength <0.1).

The average orientation vector strengths of maps evoked from the two eyes were compared at a given SF. Eyes through which lower VEP amplitudes were evoked exhibited lower average vector strengths at nearly all SFs. Pseudo-color-coded images of the vector strength per pixel (vector map) are given for A cat A7 in Fig. 5. Green and yellow colors indicating high vector strength dominate in the territory of the stronger eye compared with blue colors, which indicate lower vector strengths in the territory of the weaker eye at most of the SFs. The average vector strength per pixel in a defined region of interest was higher for the nonsquinting eye at all tested SFs in cat A7 ($18.9 \pm 16.6\%$) but not in cat A1 (mean difference, $2.7 \pm 2.4\%$; Fig. 6A). This was in good agreement with the accompanying differences in VEP amplitudes (Fig. 6, B and C).

In the group of A cats (A3–A11), the mean inter-ocular vector strength difference between orientation maps at all tested SFs (with the exception of 2.0 cycles/°) was $18.5 \pm 0.41\%$ ($n = 12$ hemispheres; Fig. 7A, Table 1). For comparison, the monocularly deprived cat exhibited an inter-ocular difference in orientation vector strength of 66% at a SF of 0.5 cycles/°. When averaging over all data sets at a certain SF (Fig. 7B), the mean vector strength difference was similar ($18 \pm 13\%$; $n = 56$ data sets, only cats A3–A9). In $86 \pm 14\%$ of the A data sets, average orientation vector strength was lower for the eye that was identified as the weaker one in the VEP measurements.

By contrast, the normal and the two NA cats exhibited relative differences between the average vector strength of the maps of different eyes of <9% at each tested SF (0.1–2.0 cycles/°). As exemplified for cat A1, these small interocular differences in vector strength (Fig. 6A) were of the same magnitude as the small VEP amplitude differences that justified the classification of this cat as NA (Fig. 6C).

Average vector strength differences were $4.4 \pm 2.4\%$ for the two NA cats and $4.6 \pm 1.9\%$ for the three normal cats (Fig. 7A, Table 1). In cats N1 and A1, the eye producing the higher vector strength per SF switched nonsystematically and not always consistently with the eye dominance in VEP recordings; each eye led in about one-half of the cases (Fig. 6, A and C). In NA cat A2, the left operated eye led in vector strength at all SFs except 0.1 cycles/° (83% of the data sets), but interocular differences were not higher than for the remaining normal/NA group. Mean vector strength differences are significantly different between cats of the normal/NA ($n = 5$) group and cats of the A ($n = 9$) group (Fig. 7A, Table 1, Mann-Whitney-U: $P = 0.0027$).

When SFs were separated, the distributions of mean vector strength differences were significantly different between the normal/NA and the A group at 0.7, 1.0, and 1.3 cycles/° (all cats except N2, N3, A10, and A11, $n = 13$ hemispheres per set, Mann-Whitney: $P < 0.05$; Fig. 7B). In agreement with the fading of the weaker eye's maps toward high SFs (Fig. 4), the difference in vector strength (group average) increased toward higher SFs in the A group. Although average interocular differences were computed from different data blocks and cats, a linear regression fit revealed a significant increase of mean vector strength differences between maps evoked through different eyes toward high SFs in the A group (ANOVA, $R = 0.3$;

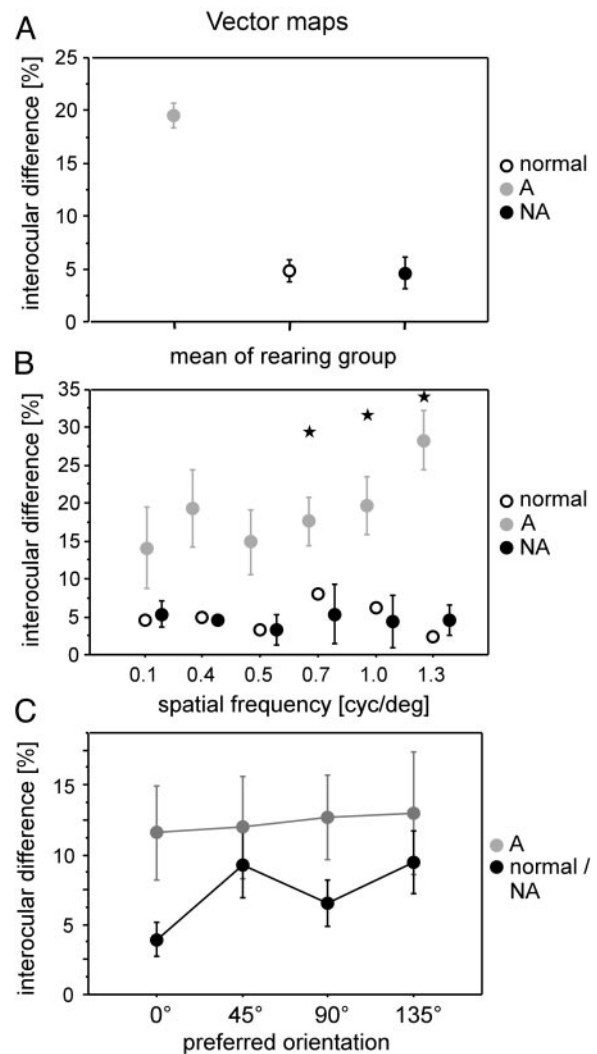


FIG. 7. Means of interocular differences in average vector strength splitted by group (A), SF (B), and angle (C). Error bars = SE. A: interocular vector strength differences in the monocular tuning maps. Means of all maps in individual cats were averaged per group as classified according to the VEP criteria (NA/A). The difference between the normal/NA group and the A group is significant ($P = 0.0027$). B: interocular vector strength differences in the monocular tuning maps split by SF and averaged by cat. Stars indicate significance ($P \leq 0.05$). C: interocular vector strength differences split by preference angle and group (all cats, data obtained at 0.5 cycles/°). Normal and NA cats show smaller differences in vertical and horizontal domains than in oblique.

$P = 0.02$) but not in the normal/NA group (ANOVA, $R = 0.059$; $P = 0.81$; Fig. 7B). Because these data originated from a composite sample, we additionally repeated the same test 100 times with randomly resampled subsets each time including 90% of the original A data. This analysis revealed a significant ($P \leq 0.05$) positive regression between interocular differences and SFs in 80% of the subsamples.

In three A cats (A4, A5, and A7), both hemispheres were investigated. In this subsample, interocular differences in vector strength were on average higher in the hemispheres contralateral ($19.1 \pm 7.6\%$) than ipsilateral ($11 \pm 6.6\%$) to the weaker eye.

Analyzing interocular vector strength differences in relation to preferred angle of orientation revealed that in maps evoked with 0.5-cycles/° differences in the normal/NA group were

usually smaller in vertical and horizontal than in oblique angle compartments. However, in the A group, the advantage of both cardinal angles diminished and interocular differences were equally high at all angles (Fig. 7C). Also, pixels preferring vertical contours did not appear to be numerically underrepresented (data not shown).

Correlation of VEP and optical imaging data

Differences in orientation vector strength were also compared with differences in mean VEP amplitudes at the respective SFs to validate that VEP amplitude differences are predictive for differences in vector strength. For this analysis, only VEP recordings from the hemisphere used for optical imaging were evaluated. This comparison revealed a significant correlation between the direction and size of the difference in VEP amplitude and the direction and size of the difference in orientation vector strength at a given SF (Fig. 8; all cats except N2, N3, A10, and A11; $n = 66$; $R = 0.619$, $P < 0.0001$).

Ocular dominance distribution

To exclude that the weaker eye dominated less cortical territory and drove less neurons, as it is the case with monocular deprivation, we investigated ocular dominance distributions both in the maps and electrophysiologically. In the optically recorded maps, ocular dominance distributions at each tested SF were estimated on a strongest-response-per-pixel basis for the respective condition cocktail. In the A group, the cortical representation of both eyes was balanced in the average of all data sets. The numbers of pixels dominated by different eyes differed by $0.8 \pm 27\%$ per cat/SF pair. The weak eye tended to dominate slightly more pixels than the normal eye at low SFs (≤ 0.4 cycles/°) and less pixels than the normal eye at high SFs (≥ 1.0 cycles/°; Fig. 9A).

The ocular dominance of single units in area 17 was assessed in A cat A7 (Fig. 9B, 141 units) and NA cat A1 (Fig. 9C, 179 units) at the end of the imaging experiments. In both cats, the fraction of binocular neurons of class 3 was drastically reduced

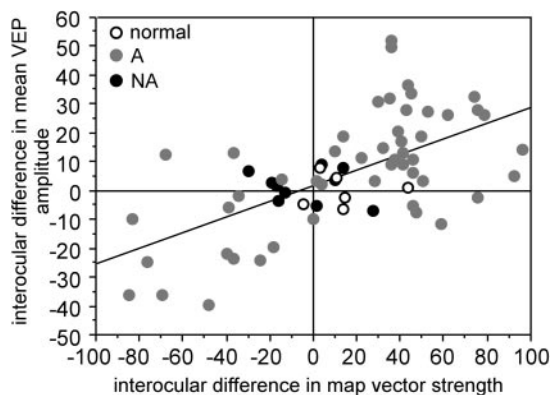


FIG. 8. Mean VEP amplitude difference per SF and cat plotted against the interocular vector strength difference in the corresponding data set of tuning maps. VEP data were taken from the electrodes placed over the respective imaged hemisphere. Positive differences indicate that the right eye was leading; negative differences indicate that the left eye was leading. Since in most of the cases the left eye was squinting, and as a consequence, was the weaker eye, most data points are in the *top right quadrant*. A significant positive relationship between VEP amplitude difference and vector strength difference can be observed ($P < 0.0001$, $R = 0.619$, $n = 66$ data sets).

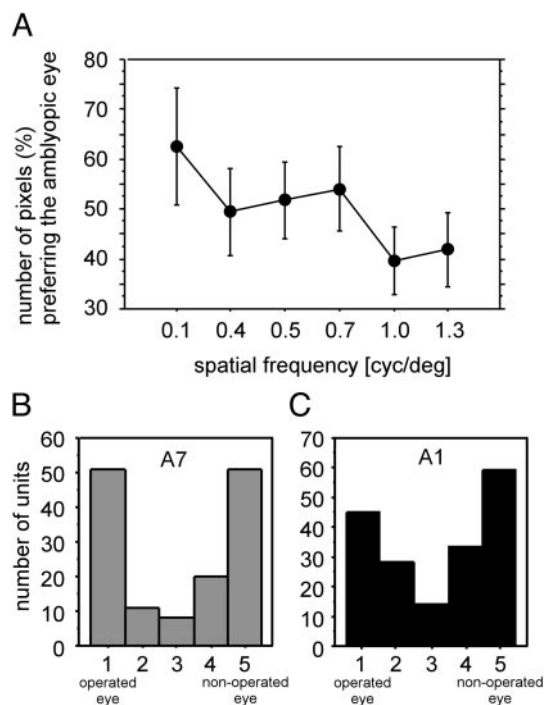


FIG. 9. Ocular dominance distributions. *A*: mean interocular difference in percentage between the number of pixels responding strongest to the weak compared with the fellow eye (all A cats are included). Error bars indicate SD. *B*: ocular dominance (OD) distributions of the strongest responses of single units recorded in V1 of the left hemispheres of cat A7 (141 units) and A1 (179 units) ipsilateral to the operated eyes. Ocular dominance was rated in 5 classes [1 and 5 represent cells monocularly driven by the ipsi- (operated) or contralateral (nonoperated) eye, 2 and 4 binocularly driven cells with a bias to the ipsi- (operated) or contralateral (nonoperated) eye, respectively; 3 represents binocular cells driven equally well by both eyes].

(A cat A8: 5.7%; NA cat A1: 7.8%) compared with the normal distribution in cat area 17. In cat A8 (A1), 36% (25%) of the neurons responded only to the operated eye and 36% (33%) responded exclusively to the normal eye in the hemisphere ipsilateral to the operated eye. Therefore we can exclude that the reduced VEP amplitudes and the reduced contrast in the orientation maps were due to a loss of neurons responding to the operated eye.

DISCUSSION

In this study, we found that responses and tuning for orientation preference of population activity in area 17 evoked by stimulation of the amblyopic eye were impaired at nearly all tested SFs. Hereby, the interocular difference in VEP amplitudes was predictive of the interocular difference in average map vector strength at the same SF and both differences increased with increasing SF.

Nevertheless, the structure of the maps of amblyopic cats was preserved as indicated by preferentially orthogonal intersection angles between orientation domains and ocular dominance borders and continuity of orientation domains over ocular dominance (OD) borders.

Validity of the observations

In this study, VEP amplitudes were taken as an objective indicator of interocular differences in visual acuity because

phase reversal and pattern VEP amplitudes correspond well with behaviorally tested visual acuity and/or contrast sensitivity in both cats and humans (Campbell and Maffei 1970; Harter and White 1967; Towle and Harter 1977). Thus VEPs were frequently used before to objectively determine visual acuity in cats (Berkley and Watkins 1971; Campbell et al. 1973; Freeman and Marg 1975; von Grünau and Singer 1980; Yin et al. 1983) and in children (e.g., Sokol 1976).

We observed deficits mainly in recordings evoked through squinting eyes and are confident that these deficits are not result of refractive errors or of deprivation amblyopia induced by the ocular trauma (Crewther et al. 1985; Ikeda and Wright 1976; Ikeda and Tremain 1979; Rauschecker 1991). First, refraction was double-checked by two experimenters. Second, both optically and electrophysiologically estimated ocular dominance distributions were balanced. Third, in one cat, the nonoperated eye developed reduced visual acuity as described previously (Cleland et al. 1982; Yin et al. 1983).

Comparison to previous studies

The geometric relationship between orientation and ocular dominance columns in the maps was preserved for both A and NA eyes. As in normal animals (Huebener et al. 1997) and divergent (Löwel et al. 1998) and convergent NA cats (Engelmann et al. 2002), orientation domains crossed ocular dominance borders continuously and at steep angles. This argues against the hypothesis that suppression of one eye during development alters the layout of the orientation map (Engelmann et al. 2002). It supports the assumption of an early stabilization of the basic layout of the orientation map that is resistant to the reorganization of both thalamocortical and intracortical connections in squinting cats (Löwel et al. 1998; Schmidt et al. 1999).

Although optical imaging captures activity of many neurons, we did not observe any reduction of neurons preferring vertical contours (Chino et al. 1991; Cynader et al. 1984; Singer et al. 1979). However, it is possible that in our study, not all orientation compartments were sampled sufficiently to allow for a pixel-based angle statistic.

Our finding of clearly reduced orientation vector strengths for the A eye at various SFs in area 17 was surprising given the controversial findings in the literature on single cell response properties in cats but matches recent observations in monkeys and humans. We observed variable interindividual degrees of interocular tuning differences (Table 1) correlating with interocular VEP amplitude differences. This is in accordance with observations in behaviorally tested anisometropic and strabismic A monkeys. These showed moderate deficits in SF tuning of single neurons that correlated with the severeness of the behavioral deficit (Kiorpes et al. 1998). The optical data also match fMRI (Algaze et al. 2002; Barnes et al. 2001; Goodyear et al. 2000, 2002) and PET (Choi et al. 2002; Demer et al. 1997; but see Imamura et al. 1997) studies in A humans, which demonstrate lower activity levels in early visual areas after stimulation of the A eye.

We have quantified the orientation vector strength, a parameter that can be interpreted as a measure of population orientation selectivity. It is theoretically independent of response strength. Thus lowering of vector strength could indicate that neurons still respond vigorously but become less selective.

However, electrophysiological evidence for a broadening of orientation selectivity in neurons dominated by A eyes is rather weak (e.g., Kalil et al. 1984; Roelfsema et al. 1993; Singer et al. 1980). Vector strength could practically be susceptible to a decrease in signal-to-noise ratio and thus to the decreased response strength of pixels dominated by the A eye (Fig. 4). Thus the impaired population tuning could be secondary to decreased responses at certain SFs. However, earlier single cell studies in cats rarely reported decreased SF tuning of neurons dominated by the amblyopic eye in central vision (Kalil et al. 1984; Mower et al. 1982; Roelfsema et al. 1994; Singer et al. 1980). There is rather evidence for reduced spatial and orientation selectivity for both eyes (Chino et al. 1983, 1991) or for the subpopulation of binocular neurons (Crewther and Crewther 1990, 1993). In the latter studies, binocular neurons were dominated by the deviating eye at low SFs and by the nondeviating eye at high SFs. This is compatible with our data indicating that weaker eyes dominate slightly more map territory than fellow eyes at low SFs and less at high SFs. In addition, we could also confirm that the amblyopic eye is contralaterally stronger impaired (Chino et al. 1990; but see Kalil et al. 1984).

In summary, both reduced spatial and orientation selectivity of neurons driven by the amblyopic eye can be responsible for our observation of decreased vector strength. The deficit seems to be more obvious in metabolic population activity than on the single cell level. This could be based on the larger sampling basis in optical imaging but may also be related to the nature of the optical signal. Optical imaging as other measurements of cerebral blood flow also captures response variables that are poorly reflected by spiking activity such as subthreshold synaptic responses (Das and Gilbert 1995; Toth et al. 1996; see also Logothetis et al. 2001; Mathiesen et al. 1998). This may also be the reason for the close correlation between vector strength and VEP amplitudes. VEPs depend on the number of active synapses impinging on dipole targets rather than on mere spiking activity. Likewise, amplitudes of evoked field potentials elicited from the deviating eye were reduced, which was attributed to enhanced latency scatter caused by intracortically impaired transmission (Singer et al. 1980; see also Eschweiler and Rauschecker 1993). Indeed, latencies of responses to the deviating eye are prolonged and more variable both after electrical (Freeman and Tsumoto 1983) and visual stimulation (Eschweiler and Rauschecker 1993; see also Chino et al. 1983), indicating a disturbed temporal structure of cortical discharges. Indications for reduced temporal precision of firing are that cells connected to A eyes cannot synchronize their responses in the millisecond range at high SFs (Roelfsema et al. 1994). Thus a disturbance in the temporal structure of synaptic, partly subthreshold, activity impinging on supragranular neurons connected to the A eye might have contributed to the impairment of optical signals.

Neuroanatomical substrate

The decrease in vector strength might be a consequence of impaired intra-areal or interareal connectivity or both. Indirect evidence is compatible with both possibilities. Tangential intrinsic connections contribute to orientation selectivity (e.g., Crook et al. 1997) and to synchronization of responses across columns (Gray et al. 1989). The latter is impaired in amblyopic

cats, suggesting abnormalities at the level of intrinsic connections (Roelfsema et al. 1994). There is no evidence that intrinsic connections in strabismic cats are quantitatively altered within the eye-specific territories (Löwel and Singer 1992; Tychsen and Burkhalter 1995; Tychsen et al. 1996), and exotropic squinters develop orientation-specific connections for both eyes (Schmidt et al. 1997). However, exotropic squinters become less frequently A than esotropic squinters (Duke-Elder and Wybar 1973), and actual data on the specificity of intrinsic connections in tested amblyopes are still lacking.

In support of the involvement of feedback connections is evidence that vector strength and response strength in orientation maps in cat areas 17 and 18 decrease when feedback from extrastriate cortex (PMLS) is blocked (Galuske et al. 2002; Schmidt et al. 2000). The number of neurons driven by the amblyopic eye in area PMLS is slightly lower than that of neurons driven by the normal eye (Schröder et al. 2002; Sireteanu and Best 1992). Therefore reduced responses in area 17 of amblyopic cats might be due to a lack of eye-specific feedback connections from PMLS where the affected eye is under-represented.

Conclusion from this study

Accepting visual acuity loss as an indicator of amblyopia, our results indicate that amblyopia is not associated with structural changes of the orientation preference maps in V1. Nevertheless, we confirm observations in monkeys and humans that cortical processing of visual information from the A eye is already disturbed at this level.

ACKNOWLEDGMENTS

The authors thank R. Goebel for the visual stimulation program, J. Hinrich-Schröder for an EP analysis tool, F. Wolf and F. Hofstätter for algorithms of map geometry analysis, S. Schwegmann for technical assistance, and M. Stephan for programming support.

GRANTS

This study was supported by the Max-Planck-Society.

REFERENCES

- Algabe A, Roberts C, Leguire L, Schmalbrock P, and Rogers G.** Functional magnetic resonance imaging as a tool for investigating amblyopia in the human visual cortex: a pilot study. *J Am Assoc Pediatr Ophthalmol Strabismus* 6: 300–308, 2002.
- Altmann L and Singer W.** Temporal integration in amblyopic vision. *Vision Res* 26: 1959–1968, 1986.
- Arden GB, Barnard WM, and Mushin AS.** Visually evoked responses in amblyopia. *Br J Ophthalmol* 58: 183–192, 1974.
- Barnes GR, Hess RF, Dumoulin SO, Achtman RL, and Pike GB.** The cortical deficit in humans with strabismic amblyopia. *J Physiol* 533: 281–297, 2001.
- Berkley MA and Watkins DW.** Visual acuity of the cat estimated from evoked cerebral potentials. *Nature* 234: 91–92, 1971.
- Blakemore C and Vital-Durand F.** Different neural origins for ‘blur’ amblyopia and strabismic amblyopia. *Ophthalmol Physiol Opt* 12:83, 1992.
- Bonhoeffer T and Grinvald A.** The layout of iso-orientation domains in area 17 of cat visual cortex: optical imaging reveals a pinwheel-like organization. *J Neurosci* 13: 4157–4180, 1993.
- Campbell FW and Maffei L.** Electrophysiological evidence for the existence of orientation and size detectors in the human visual system. *J Physiol* 207: 635–652, 1970.
- Campbell FW, Maffei L, and Piccolino M.** The contrast sensitivity of the cat. *J Physiol* 229: 719–731, 1973.
- Chino YM, Ridder WH III, and Czora EP.** Effects of convergent strabismus on spatio-temporal response properties of neurons in cat area 18. *Exp Brain Res* 72: 264–278, 1988.
- Chino YM, Shansky MS, Jankowski WL, and Banser FA.** Effects of rearing kittens with convergent strabismus on development of receptive-field properties in striate cortex neurons. *J Neurophysiol* 50: 265–286, 1983.
- Chino YM, Smith EL III, Wada H, Ridder WH III, Langston AL, and Leshner GA.** Disruption of binocularly correlated signals alters the postnatal development of spatial properties in cat striate cortical neurons. *J Neurophysiol* 65: 841–859, 1991.
- Choi MY, Lee DS, Hwang JM, Choi DG, Lee KM, Park KH, and Yu YS.** Characteristics of glucose metabolism in the visual cortex of amblyopes using positron-emission tomography and statistical parametric mapping. *J Pediatr Ophthalmol Strabismus* 39: 11–19, 2002.
- Cleland BG, Crewther DP, Crewther SG, and Mitchell DE.** Normality of spatial resolution of retinal ganglion cells in cats with strabismic amblyopia. *J Physiol* 326: 235–249, 1982.
- Crawford ML, von Noorden GK, Meharg LS, Rhodes JW, Harwerth RS, Smith EL III, and Miller DD.** Binocular neurons and binocular function in monkeys and children. *Invest Ophthalmol Vis Sci* 24: 491–495, 1983.
- Crewther DP and Crewther SG.** Neural site of strabismic amblyopia in cats: spatial frequency deficit in primary cortical neurons. *Exp Brain Res* 79: 615–622, 1990.
- Crewther SG and Crewther DP.** Amblyopia and suppression in binocular cortical neurons of strabismic cat. *Neuroreport* 4: 1083–1086, 1993.
- Crewther SG, Crewther DP, and Cleland BG.** Convergent strabismic amblyopia in cats. *Exp Brain Res* 60: 1–9, 1985.
- Crook JM, Kisvarday ZF, and Eysel UT.** GABA-induced inactivation of functionally characterized sites in cat striate cortex: effects on orientation tuning and direction selectivity. *Vis Neurosci* 14: 141–158, 1997.
- Cynader M, Gardner JC, and Mustari M.** Effects of neonatally induced strabismus on binocular responses in cat area 18. *Exp Brain Res* 53: 384–399, 1984.
- Das A and Gilbert CD.** Long-range horizontal connections and their role in cortical reorganization revealed by optical recording of cat primary visual cortex. *Nature* 375: 780–784, 1995.
- Demer JL, Grafton S, Marg E, Mazziotta JC, and Nuwer M.** Positron-emission tomographic study of human amblyopia with use of defined visual stimuli. *J Am Assoc Pediatr Ophthalmol Strabismus* 1: 158–171, 1997.
- Duke-Elder S and Wybar K.** System of ophthalmology. In: *Ocular Motility and Strabismus*, edited by Duke-Elder S. London: Kimpton, 1973, p. 270–317.
- Engelmann R, Crook JM, and Lowel S.** Optical imaging of orientation and ocular dominance maps in area 17 of cats with convergent strabismus. *Vis Neurosci* 19: 39–49, 2002.
- Eschweiler GW and Rauschecker JP.** Temporal integration in visual cortex of cats with surgically induced strabismus. *Eur J Neurosci* 5: 1501–1509, 1993.
- Freeman DN and Marg E.** Visual acuity development coincides with the sensitive period in kittens. *Nature* 254: 614–615, 1975.
- Freeman RD, Sclar G, and Ohzawa I.** An electrophysiological comparison of convergent and divergent strabismus in the cat: visual evoked potentials. *J Neurophysiol* 49: 227–237, 1983.
- Freeman RD and Tsumoto T.** An electrophysiological comparison of convergent and divergent strabismus in the cat: electrical and visual activation of single cortical cells. *J Neurophysiol* 49: 238–253, 1983.
- Galuske RAW, Kim D-S, Castren E, and Singer W.** Differential effects of neurotrophins on ocular dominance plasticity in developing and adult cat visual cortex. *Eur J Neurosci* 12: 3315–3330, 2000.
- Galuske RAW, Schmidt KE, Goebel R, Lomber SG, and Payne BR.** The role of feedback in shaping neural representations in visual cortex. *Proc Natl Acad Sci USA* 99: 17083–17088, 2002.
- Goodyear BG, Nicolle DA, Humphrey GK, and Menon RS.** BOLD fMRI response of early visual areas to perceived contrast in human amblyopia. *J Neurophysiol* 84: 1907–1913, 2000.
- Goodyear BG, Nicolle DA, and Menon RS.** High resolution fMRI of ocular dominance columns within the visual cortex of human amblyopes. *Strabismus* 10: 129–136, 2002.
- Gray CM, König P, Engel AK, and Singer W.** Oscillatory responses in cat visual cortex exhibit inter-columnar synchronization which reflects global stimulus properties. *Nature* 338: 334–337, 1989.
- Gu Q and Singer W.** Effects of intracortical infusion of anticholinergic drugs on neuronal plasticity in kitten striate cortex. *Eur J Neurosci* 5: 475–485, 1993.

- Harter MR and White CT.** Perceived number and evoked cortical potentials. *Science* 156: 406–408, 1967.
- Hess RF, Campbell FW, and Greenhalgh T.** On the nature of the neural abnormality in human amblyopia; neural aberrations and neural sensitivity loss. *Pfluegers Arch* 377: 201–207, 1978.
- Hess RF and Holliday IE.** The spatial localization deficit in amblyopia. *Vision* 32: 1319–1339, 1992.
- Hohmann A and Creutzfeldt OD.** Squint and the development of binocularity in humans. *Nature* 254: 613–614, 1975.
- Holopigian K, Seiple W, and Kupersmith M.** VEP threshold and supra-threshold deficits in amblyopia. *Clin Vision Sci* 6: 109–117, 1991.
- Horton JC and Hocking DR.** Pattern of ocular dominance columns in human striate cortex in strabismic amblyopia. *Vis Neurosci* 13: 787–795, 1996.
- Hubel DH and Wiesel TN.** Binocular interaction in striate cortex of kittens reared with artificial squint. *J Neurophysiol* 28: 1041–1059, 1965.
- Hubener M, Shoham D, Grinvald A, and Bonhoeffer T.** Spatial relationships among three columnar systems in cat area 17. *J Neurosci* 17: 9270–9284, 1997.
- Ikeda H and Tremain KE.** Amblyopia occurs in retinal ganglion cells in cats reared with convergent squint without alternating fixation. *Exp Brain Res* 35: 559–582, 1979.
- Ikeda H and Wright MJ.** Properties of LGN cells in kittens reared with convergent squint: a neurophysiological demonstration of amblyopia. *Exp Brain Res* 25: 63–77, 1976.
- Imamura K, Richter H, Fischer H, Lennerstrand G, Franzen O, Rydberg A, Andersson J, Schneider H, Onoe H, Watanabe Y, and Langström B.** Reduced activity in the extrastriate visual cortex of individuals with strabismic amblyopia. *Neurosci Lett* 225: 173–176, 1997.
- Issa NP, Trepel C, and Stryker MP.** Spatial frequency maps in cat visual cortex. *J Neurosci* 20: 8504–8514, 2000.
- Kalil RE, Spear PD, and Langsetmo A.** Response properties of striate cortex neurons in cats raised with divergent or convergent strabismus. *J Neurophysiol* 52: 514–537, 1984.
- Kiorpes L, Kiper DC, O'Keefe LP, Cavanaugh JR, and Movshon JA.** Neuronal correlates of amblyopia in the visual cortex of macaque monkeys with experimental strabismus and anisometropia. *J Neurosci* 18: 6411–6424, 1998.
- Lagreze WD and Sireteanu R.** Two-dimensional spatial distortions in human strabismic amblyopia. *Vision Res* 31: 1271–1288, 1991.
- Levi DM and Harwerth RS.** Contrast evoked potentials in strabismic and anisometric amblyopia. *Invest Ophthalmol Vis Sci* 17: 571–575, 1978.
- Levi DM and Klein SA.** Spatial localization in normal and amblyopic vision. *Vision Res* 23: 1005–1017, 1983.
- Levi DM and Klein SA.** Vernier acuity, crowding and amblyopia. *Vision Res* 25: 979–991, 1985.
- Logothetis NK, Pauls J, Augath M, Trinath T, and Oeltermann A.** Neurophysiological investigation of the basis of the fMRI signal. *Nature* 412: 150–157, 2001.
- Lombroso CT, Duffy FH, and Robb RM.** Selective suppression of cerebral evoked potentials to patterned light in amblyopia ex anopsia. *Electroencephalogr Clin Neurophysiol* 27: 238–247, 1969.
- Löwel S.** Ocular dominance column development: strabismus changes the spacing of adjacent columns in cat visual cortex. *J Neurosci* 14: 7451–7468, 1994.
- Löwel S and Engelmann R.** Neuroanatomical and neurophysiological consequences of strabismus: changes in the structural and functional organization of the primary visual cortex in cats with alternating fixation and strabismic amblyopia. *Strabismus* 10: 95–105, 2002.
- Löwel S, Schmidt KE, Kim DS, Wolf F, Hoffsummer F, Singer W, and Bonhoeffer T.** The layout of orientation and ocular dominance domains in area 17 of strabismic cats. *Eur J Neurosci* 10: 2629–2643, 1998.
- Löwel S and Singer W.** Selection of intrinsic horizontal connections in the visual cortex by correlated neuronal activity. *Science* 255: 209–212, 1992.
- Manny RE and Levi DM.** The visually evoked potential in humans with amblyopia: pseudorandom modulation of uniform field and sine-wave gratings. *Exp Brain Res* 47: 15–27, 1982.
- Mathiesen C, Caesar K, Akgoren N, and Lauritzen M.** Modification of activity-dependent increases of cerebellar blood flow by excitatory synaptic activity and spikes in rat cerebellar cortex. *J Physiol* 512: 555–566, 1998.
- Mower GD, Burchfiel JL, and Duffy FH.** Animal models of strabismic amblyopia: physiological studies of visual cortex and the lateral geniculate nucleus. *Dev Brain Res* 281: 311–327, 1982.
- Olson CR and Freeman R.** Eye alignment in kittens. *J Neurophysiol* 41: 848–859, 1978.
- Pugh M.** Visual distortion in amblyopia. *Br J Ophthalmol* 42: 449–460, 1958.
- Rauschecker JP.** Mechanisms of visual plasticity: Hebb synapses, NMDA receptors, and beyond. *Physiol Rev* 71: 587–615, 1991.
- Roelfsema PR, Konig P, Engel AK, Sireteanu R, and Singer W.** Reduced synchronization in the visual cortex of cats with strabismic amblyopia. *Eur J Neurosci* 6: 1645–1655, 1994.
- Schmidt KE, Galuske RAW, and Singer W.** Matching the modules: cortical maps and long-range intrinsic connections in visual cortex during development. *J Neurobiol* 41: 10–17, 1999.
- Schmidt KE, Goebel R, Castelo-Branco M, Lomber SG, Payne BR, and Galuske RAW.** Global motion representation in cat primary visual cortex and its emergence based on feedback connections. *Soc Neurosci Abstr* 26: 162.3, 2000.
- Schmidt KE, Kim DS, Singer W, Bonhoeffer T, and Löwel S.** Functional specificity of long-range intrinsic and interhemispheric connections in the visual cortex of strabismic cats. *J Neurosci* 17: 5480–5492, 1997.
- Schröder JH, Fries P, Roelfsema PR, Singer W, and Engel AK.** Ocular dominance in extrastriate cortex of strabismic amblyopic cats. *Vision Res* 42: 29–39, 2002.
- Shatz CJ, Lindstrom S, and Wiesel TN.** The distribution of afferents representing the right and left eyes in the cat's visual cortex. *Brain Res* 131: 103–116, 1977.
- Sherman S.** Development of interocular alignment in cats. *Brain Res* 37: 187–203, 1972.
- Singer W, von Grünau M, and Rauschecker J.** Requirements for the disruption of binocularity in the visual cortex of strabismic kittens. *Brain Res* 171: 536–540, 1979.
- Singer W, von Grünau M, and Rauschecker J.** Functional amblyopia in kittens with unilateral exotropia. I. Electrophysiological assessment. *Exp Brain Res* 40: 294–304, 1980.
- Sireteanu R and Best J.** Squint-induced modification of visual receptive fields in the lateral suprasylvian cortex of the cat: binocular interaction, vertical effect and anomalous correspondence. *Eur J Neurosci* 4: 235–242, 1992.
- Sireteanu R, Lagreze WD, and Constantinescu DH.** Distortions in two-dimensional visual space perception in strabismic observers. *Vision Res* 33: 677–690, 1993a.
- Sireteanu R, Singer W, Fronius M, Greuel JM, Best J, Fiorentini A, Bisti S, Schiavi C, and Campos E.** Eye alignment and cortical binocularity in strabismic kittens: a comparison between tenotomy and recession. *Vis Neurosci* 10: 541–549, 1993b.
- Snyder A and Shapley R.** Deficits in the visual evoked potentials of cats as a result of visual deprivation. *Exp Brain Res* 37: 73–86, 1979.
- Sokol S.** Visually evoked potentials: theory, techniques and clinical applications. *Surv Ophthalmol* 21: 18–44, 1976.
- Spekreijse H, van der Tweel LH, and Khoe L.** Electrophysiology and psychophysics of a case of amblyopia. *Vision Res* 11: 1205, 1971.
- Thompson JK, Peterson MR, and Freeman RD.** Single-neuron activity and tissue oxygenation in the cerebral cortex. *Science* 299: 1070–1072, 2003.
- Toth LJ, Rao SC, Kim D-S, Somers D, and Sur M.** Subthreshold facilitation and suppression in primary visual cortex revealed by intrinsic signal imaging. *Proc Natl Acad Sci USA* 93: 9869–9874, 1996.
- Towle VL and Harter MR.** Objective determination of human visual acuity: pattern evoked potentials. *Invest Ophthalmol Vis Sci* 16: 1073–1076, 1977.
- Trachtenberg JT and Stryker MP.** Rapid anatomical plasticity of horizontal connections in the developing visual cortex. *J Neurosci* 21: 3476–3482, 2001.
- Tychsen L and Burkhalter A.** Neuroanatomic abnormalities of primary visual cortex in macaque monkeys with infantile esotropia: preliminary results. *J Pediatr Ophthalmol* 32: 323–328, 1995.
- Tychsen L, Burkhalter A, and Bothe RG.** Functional and structural abnormalities in the visual cortex in early childhood strabismus. *Klin Monatsbl Augenheilkd* 208: 18–22, 1996.
- Von Grünau MW.** The role of maturation and visual experience in the development of eye alignment in cats. *Exp Brain Res* 37: 41–47, 1979.
- Von Grünau MW and Singer W.** Functional amblyopia in kittens with unilateral exotropia. II. Correspondence between behavioural and electrophysiological assessment. *Exp Brain Res* 40: 305–310, 1980.
- Yin TC, Kalil RE, and Schechter PB.** Visual-evoked responses from strabismic cats. A comparison of esotropes with exotropes. *Invest Ophthalmol Vis Sci* 24: 1390–1399, 1983.
- Yin ZQ, Li CY, Pei X, Vaegan, and Fang QX.** Development of pattern ERG and pattern VEP spatial resolution in kittens with unilateral esotropia. *Invest Ophthalmol Vis Sci* 35: 626–634, 1994.